Interaction Notes

Note 465

May 1988

Commonalities in the SEM Parameters of Several Simple Thin Wire Geometries

Lloyd S. Riggs
John M. Lindsey
Thomas H. Shumpert
Electrical Engineering
Auburn University, AL 36849

Abstract

The Singularity Expansion Method (SEM) parameters (natural frequencies, natural modes, and coupling coefficients) are presented for several different geometries each composed of four arbitrarily-oriented, thin, straight wire scatterers with one end of each of the four straight members connected at a common intersection point. Various choices of the orientations (and lengths) of these four members result in specific configurations which have been investigated previously (perpendicular crossed wires, planar symmetric tri-arm, L-shaped wire, and straight wire) as well as several other configurations which have not (nonplanar symmetric and nonsymmetric tetra-arms, nonplanar symmetric and nonsymmetric tri-arms, and arbitrarily bent wire). The SEM parameters for the general tetra-arm structure are calculated for a wide range of geometrical configurations. Commonalities which exist between the SEM parameters of the general tetra-arm scatterer and the previously analyzed "dipoles", "tripoles" and "crossed dipoles" are presented and discussed. These data suggest that the SEM parameters of some of the more complicated scattering structures may be expressed partially as (or decomposed into) combinations of the SEM parameters of several simpler geometrical configurations.

I. Introduction

The Singularity Expansion Method (SEM) has proven to be a powerful analytical (and numerical) tool providing significant insight into the fundamental behavior of electromagnetic radiators (antennas) and reradiators (scatterers). The SEM data presented in the simple analyses and comparisons addressed in this paper indicate that it is possible (at least in some specific classes of antenna and scattering problems) to express some of the SEM parameters of a more complicated geometrical structure in terms of the SEM parameters of simpler structures which may be geometrically combined to form the original structure of interest. However, it should be noted that the interaction of these various simpler decomposition structures is not included in the SEM parameters thus obtained.

One of these postulated cases of decomposition will be demonstrated by determining the SEM parameters for a general four-arm (subsequently referred to as tetra-arm) scatterer excited by an arbitrarily-polarized, arbitrarily-oriented incident plane wave. The calculated SEM parameters of the general tetra-arm scatterer will be compared to those SEM parameters previously determined for several specific scattering geometries such as the straight wire [1], the L-shaped wire [2], the planar symmetric tri-arm scattering element [3], and the perpendicular crossed wires [4]. Commonalities of the various SEM parameters of these previously analyzed scattering structures and the general tetra-arm scattering elements are presented. Also addressed is the very intriguing special case of the nonplanar symmetric tetra-arm scatterer which possesses the unique symmetry that the distance from the tip of each arm of this tetra-arm scatterer to the tip of any other arm is constant, i.e. line segments connecting the four tips outline the simplest of the regular polyhedra, the tetrahedron.

II. Singularity Expansion Method (SEM) / Method of Moments (MOM) Formulation

Consider the perfectly conducting, thin wire tetra-arm scatterer as shown in Figure 1. In general, the specific geometry will depend on the geometrical parameters associated with each of the arms : ℓ_k , θ_k , ϕ_k , and a_k for k = 1 to 4. The electric field of the exciting plane wave is of unit

amplitude, E-field polarization orientation θ_p, ϕ_p, and is incident from the θ_{inc},ϕ_{inc} direction. Currents and charges are induced (in general) by the incident field on each of the four arms. These induced currents and charges reradiate a scattered electromagnetic field. Boundary conditions require that the superposition of the incident field and the reradiated (scattered) field vanish at every point on the surface of the tetra-arm scatterer. Using standard potential theory [5], the scattered electric field can be expressed in terms of an integro-differential operation on the induced surface current and charge. This relationship and the boundary conditions result in an electric field integral equation (EFIE) in terms of the unknown surface current on the scattering structure.

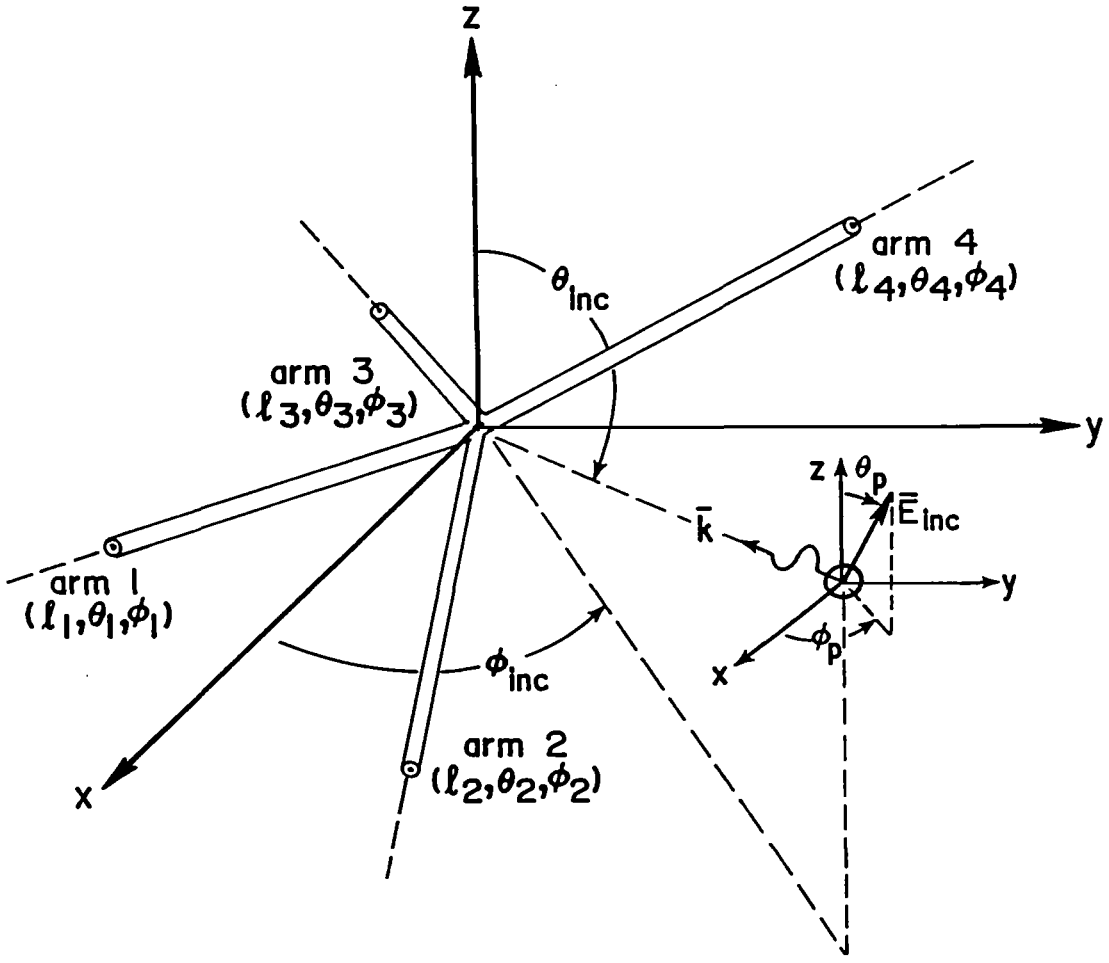

Figure 1. General Thin-Wire Tetra-Arm Scatterer Geometry with Incident Field Excitation.

This EFIE is reduced to a set of linear equations through the application of the method of moments. In particular, a Galerkin procedure, where both the expansion and testing functions have been chosen as constant pulse functions, was used in the generation of all of the data presented here. The form of the matrix equations (showing the dependence on the complex frequency variable, $s \equiv \Omega + j\omega$, explicitly) is

$$\bar{\bar{Z}}(s)\ \bar{I}(s) = \bar{V}(s) \qquad (1)$$

where

$\bar{\bar{Z}}(s) \equiv$ system impedance matrix

$\bar{I}(s) \equiv$ unknown current coefficient vector

$\bar{V}(s) \equiv$ voltage excitation vector

A typical element of $\bar{I}(s)$, i.e. $i_m(s)$, represents the Laplace transformed current at the mth zone on the tetra-arm scatterer. Similarly, an element of the excitation vector $\bar{V}(s)$, i.e. $v_n(s)$, represents a zone length times the tangential component of the incident electric field (a voltage) at the nth zone on the tetra-arm scatterer. An element of $\bar{\bar{Z}}(s)$, i.e. $z_{m,n}(s)$, gives the contribution to the voltage at the nth zone from an assumed unit current on the mth zone. Equation (1) essentially states that the current distribution on the body must be of such a form that the incident voltage at any zone on the scatterer is exactly canceled by the sum of the voltages at that zone caused by the currents in that zone and in all of the other zones on the tetra-arm scatterer.

Since the system admittance matrix is the inverse of $\bar{\bar{Z}}(s)$, poles of the response become those complex frequencies which drive the determinant of $\bar{\bar{Z}}(s)$ to zero. These poles are the natural frequencies of the scatterer since they are the frequencies for which the body can have a response (in Laplace frequency domain) with no excitation in the form of an incident wave. Poles must occur in the left-hand portion of the complex plane to insure a decaying response, and except for poles on the real axis, they must occur in conjugate pairs to insure a real time domain current or charge induced on the scatterer. Since the body loses energy due to radiation (or scatter), no poles may reside on the $j\omega$ axis.

The induced current on the radiator (or scatterer) may be expressed in the Laplace domain as [6]

$$\bar{I}(s) = f(s) \sum_{\alpha} \frac{\bar{M}_{\alpha}}{s-s_{\alpha}} \beta_{\alpha} \bar{M}_{\alpha}^{t} \bar{\Lambda}(s) \qquad (2)$$

which may be rewritten as

$$\bar{I}(s) = f(s) \sum_{\alpha} c_{\alpha}(s) \frac{\bar{M}_{\alpha}}{s-s_{\alpha}} \qquad (3)$$

with

s ≡ the complex frequency of interest

s_{α} ≡ the αth natural resonant frequency

$f(s)$ ≡ the functional form of the excitation { $f(s) = s^{-1}$ for a step function }

$\bar{\Lambda}(s)$ ≡ the vector impulsive excitation { $\bar{V}(s) = f(s)\,\bar{\Lambda}(s)$ }

$\bar{M}_{\alpha}$ ≡ the αth natural mode vector (normalized such that the complex magnitude of the largest element of $\bar{M}_{\alpha}$ is unity)

$\bar{M}_{\alpha}^{t}$ ≡ the transpose of the αth mode vector

β_{α} ≡ the normalization constant { $\beta_{\alpha}^{-1} = \bar{M}_{\alpha}^{t} \left[\frac{d\bar{\bar{Z}}}{ds}\right]_{s=s_{\alpha}} \bar{M}_{\alpha}$ }

$c_{\alpha}(s)$ ≡ the coupling coefficient { $c_{\alpha}(s) = \beta_{\alpha} \bar{M}_{\alpha}^{t} \bar{\Lambda}(s)$ }

In the next section, the various SEM parameters as defined above are given for several specific thin-wire scatterer geometries and comparisons of the commonalities of these parameters for these various configurations are made.

III. Numerical Results (Comparisons of SEM Parameters of Several Geometries)

Several different scatterer geometries are to be analyzed using the SEM approach, and the pertinent SEM parameters of these various geometries are to be presented and compared. All of these various geometries may be defined from the general geometry shown in Figure 1. Subsequently, the general scatterer as defined by this figure will be referred to as the general 4-arm star configuration. A number of specific scatterers which have been

previously analyzed using the SEM may be considered as special cases of the general 4-arm star. These various cases are: (I) isolated straight wire, ($\ell_1=\ell_2=L/2$, $a_1=a_2=a$, $\theta_1=\theta_2=\pi/2$, $\phi_1=0$, and $\phi_2=\pi$), (II) isolated bent wire, ($\ell_1= L/2$, $\ell_2= L/2$, $a_1=a_2=a$, $\theta_1=\theta_2=\pi/2$, $\phi_1=0$, and $\phi_2=\xi$ where ξ is the bend angle, $\xi=\pi$ is case (1) and $\xi=\pi/2$ or $\xi=3\pi/2$ is the L-wire),(III) planar symmetric tri-arm, ($\ell_1=\ell_2=\ell_3=L/2$, $a_1=a_2=a_3=a$, $\theta_1=\theta_2=\theta_3=\pi/2$, $\phi_1=0$, $\phi_2=2\pi/3$, and $\phi_3=4\pi/3$), (IV) planar symmetric crossed wires or tetra-arm, ($\ell_1=\ell_2=\ell_3=\ell_4=L/2$, $a_1=a_2=a_3=a_4=a$, $\theta_1=\theta_2=\theta_3=\theta_4=\pi/2$, $\phi_1=0$, $\phi_2=\pi/2$, $\phi_3=\pi$, and $\phi_4=3\pi/2$). Two additional cases of interest which will be addressed are: (V) nonplanar pseudo-symmetric tri-arm, ($\ell_1=\ell_2=\ell_3= L/2$, $a_1=a_2=a_3=a$, $\theta_1=\theta_2=\theta_3=0.392\pi$, $\phi_1=0$, $\phi_2=2\pi/3$, and $\phi_3=4\pi/3$ where $\xi=0.608\pi$ is the common bend angle), and (VI) nonplanar symmetric tetra-arm, ($\ell_1=\ell_2=\ell_3=\ell_4=L/2$, $a_1=a_2=a_3=a_4=a$, $\theta_1=\theta_3=0.696\pi$, $\theta_2=\theta_4=0.304\pi$, $\phi_1=0$, $\phi_2=\pi/2$, $\phi_3=\pi$, and $\phi_4=3\pi/2$ where $\xi=0.608\pi$ is the common bend angle between each of the four arms).

The SEM parameters (natural frequencies, natural modes, and coupling coefficients) have been determined for the six cases defined above using the methods outlined in Section II. In all of the data to be presented subsequently in this paper, the two parameters, the length-to-radius ratio (L/a = 200) and the number of moment method zones (N/L = 60) remain constant throughout the data. Table 1 presents the first several natural frequencies for the six specific scattering geometries defined above. Figures 2-4 show plots of the natural modes which accompany the fundamental and second harmonic natural frequencies given in Table 1. Figures 5-8 present coupling coefficients for these natural modes produced by linearly polarized unit amplitude plane waves incident at specific angles of interest.

Rather than comment specifically on each element of the data presented in Table 1 and Figures 2-8, it is the purpose of this paper to point out the various commonalities which exist in the data and to suggest that such commonalities represent a simple way to view the more geometrically complicated scattering structures as combinations of simpler geometries.

First it is interesting to observe that some of the natural frequencies (and concomitant natural mode vectors) of Case (IV) (see #1, #2, #5, and #6) are identical to some of those found in Case (I) (see #1 and #3). (This has been pointed out by several investigators previously [4 , 7, 8]).

Table 1. Comparisons of Natural Frequencies (sL/c) for Several Geometries of Interest.

I. Isolated Straight Wire		II. Isolated Bent Wire	
(1)	-0.257 ± j2.875	(1) -0.257 ± j2.875	($\xi=\pi$)
		(2) -0.220 ± j2.946	($\xi=2\pi/3$)
		(3) -0.205 ± j2.975	($\xi=0.608\pi$)
		(4) -0.174 ± j3.043	($\xi=\pi/2$)
(2)	-0.379 ± j5.934	(5) -0.379 ± j5.934	($\xi=\pi$)
		(6) -0.443 ± j6.049	($\xi=2\pi/3$)
		(7) -0.484 ± j6.090	($\xi=0.608\pi$)
		(8) -0.611 ± j6.160	($\xi=\pi/2$)
(3)	-0.466 ± j9.012	(9) -0.466 ± j9.012	($\xi=\pi$)
		(10) -0.502 ± j9.207	($\xi=2\pi/3$)
		(11) -0.534 ± j9.264	($\xi=0.608\pi$)
		(12) -0.616 ± j9.334	($\xi=\pi/2$)
III. Planar Symmetric Tri-Arm		**IV. Planar Symmetric Tetra-Arm**	
(1)	-0.220 ± j2.946 ($\xi=2\pi/3$)	(1) -0.257 ± j2.875	
(2)	-0.220 ± j2.946	(2) -0.257 ± j2.875	($\xi=\pi/2$)
		(3) -0.042 ± j3.220	
(3)	-0.274 ± j6.322 ($\xi=2\pi/3$)	(4) -0.313 ± j6.672	($\xi=\pi/2$)
(4)	-0.502 ± j9.207 ($\xi=2\pi/3$)	(5) -0.466 ± j9.012	
(5)	-0.502 ± j9.207	(6) -0.466 ± j9.012	($\xi=\pi/2$)
		(7) -0.589 ± j9.771	
V. Nonplanar Symmetric Tri-Arm		**VI. Nonplanar Symmetric Tetra-Arm**	
(1)	-0.205 ± j2.975 ($\xi=.608\pi$)	(1) -0.205 ± j2.975	
(2)	-0.205 ± j2.975	(2) -0.205 ± j2.975	($\xi=0.608\pi$)
(3)	-0.174 ± j3.043 ($\xi=\pi/2$)	(3) -0.205 ± j2.975	
(4)	-0.174 ± j3.043		
(5)	-0.330 ± j6.412 ($\xi=.608\pi$)	(4) -0.167 ± j6.644	($\xi=0.608\pi$)
(6)	-0.538 ± j6.610 ($\xi=\pi/2$)		
(7)	-0.534 ± j9.264 ($\xi=.608\pi$)	(5) -0.534 ± j9.264	
(8)	-0.534 ± j9.264	(6) -0.534 ± j9.264	($\xi=0.608\pi$)
(9)	-0.617 ± j9.334 ($\xi=\pi/2$)	(7) -0.534 ± j9.254	
(10)	-0.617 ± j9.334		

For certain unique excitation conditions, the "crooked mode" of the crossed wires is not excited. When this happens, the frequencies and modes which are excited are simply those of the isolated straight wire. Specific excitations produce identically zero current on some but not all of the scatterer arms.

This interesting observation was pointed out quite explicitly by Baum several years ago [9], and it has been elaborated on and identified most recently [10,11] as a spatial (or "modal") filtering technique for efficiently describing, differentiating, and categorizing unique classes or sets of geometric (as well as electrical) similarities and degeneracies. In these analyses, Baum et al. have identified the situations where certain modes of the scattering structure(s) may or may not be excited in terms of scattering structure modes (and excitations) which are symmetric or antisymmetric to some convenient (and in many cases obvious) plane of symmetry. The designation as symmetric modes in this referenced work corresponds directly to the excitation scenario where only the "crooked mode" is produced in geometries such as the crossed wire. Likewise, excitation situations which result in identically zero currents on one or more extensive regions of a scatterer correspond to the aforementioned antisymmetric modes. However, in this paper, the symmetric mode distributions will be labeled as "crooked mode" cases and antisymmetric modes will be labeled as "zero mode" cases for convenience and consistency with the other analyses of specific scattering geometries previously cited.

Another careful look at Table 1 reveals that some of the natural frequencies (and concomitant modes) of Case (III) (see #1, #2, #4, and #5) are identical to some of those found in Case (II) (see #2 and #10). Again it may be pointed out that for certain unique excitation conditions, the "zero mode" of the planar symmetric tri-arm is simply the mode of a bent wire with a bend angle of $2\pi/3$ (120°). Additional calculations not included here indicate that the "zero mode" natural frequencies (and associated natural mode functions) for the nonplanar symmetric tri-arm geometry (this additional geometry results when the three arms defined in Case (III) are pivoted toward the +z-axis by equal angles with the common pivot point remaining at the origin) are identical to those observed in the isolated bent wire case for the appropriate geometrical parameters choice. Direct evidence of this for one specific choice of angles is discussed below.

Additional commonalities apparent in Table 1 relate Case (V) (see #1, #2, #7, and #8) where $\xi=0.608\pi$ ($109.^{\circ}5$) to Case (II) (see #3 and #11) where $\xi=0.608\pi$ ($109.^{\circ}5$). Again the symmetry of the nonplanar tri-arm geometry exhibits "zero mode" natural frequencies which are identical to those of the appropriate isolated bent wire.

Another common set of data in Table 1 exist between Case (VI) (see #1, #2, #3, #5, #6, and #7) where $\xi=0.608\pi$ ($109.^{\circ}5$), Case (V) (see #1, #2, #7, and #8) where $\xi=0.608\pi$ ($109.^{\circ}5$), and Case (II) (see #3 and #11). This is a most interesting situation because if one examines the natural mode functions for the nonplanar symmetric tetra-arm scatterer, two "zero mode" vectors are found. However, neither of these "zero mode" vectors alone can account for the commonality found with the nonplanar symmetric tri-arm structure. This is easily explained if one observes that the sum of one of these "zero modes" and the "crooked mode" (both of which possess the same degenerate resonant frequencies) produces nonzero current on only three of the four arms, thus mimicking the the behavior of a three-arm scatterer. Thus some of the natural frequencies of the nonplanar symmetric tetra-arm are identical to those of the simpler structures although the natural modes of the more complicated structure are not those of the simpler structures.

A final set of common frequencies (and associated modes) are given in Table 2 along with other natural frequency data for an interesting geometrical tetra-arm configuration which may be described as a modification of Case (IV) where the two arms lying along the $\pm$x-axes are pivoted up toward the +z-axis (ϕ_1 and ϕ_3 remain the same as defined in Case (IV)) and the two arms lying along the $\pm$y-axes are pivoted down toward the -z-axis (ϕ_2 and ϕ_4 remain the same as defined in Case (IV)). It may be observed from Table 2 that when the pivot angle is 0.16667π (30°), the zero mode natural frequencies of the tetra-arm are identical to those given in Table 1 (Case (II), #2 and #10) for $\xi=2\pi/3$ (120°). Similarly, when the pivot angle is 0.19591π ($35.^{\circ}264$), the zero mode natural frequencies of the tetra-arm are identical to those given in Table 1 (Case (II), #3 and #11) for $\xi=0.608\pi$ ($109.^{\circ}47$), and when the pivot angle is 0.25π (45°), the zero mode natural frequencies of the tetra-arm are identical to those given in Table 1 (Case (II), #4 and #12) for $\xi=\pi/2$ (90°). Indeed, it may be stated (and observed in Table 2) that the zero mode natural frequencies for each of the tetra-arm cases are

Table 2. Natural Frequencies (sL/c) of the Nonplanar Symmetric Tetra-Arm.

Pivot Angle rad/(deg)	zero# mode / crooked mode	second harmonic	zero# mode / crooked mode
0 (0°)	-0.257 ± j2.875 -0.042 ± j3.220	-0.313 ± j6.672	-0.466 ± j9.012 -0.589 ± j9.771
0.02778π (5°)	-0.256 ± j2.876 -0.047 + j3.214	-0.306 ± j6.671	-0.466 ± j9.018 -0.595 ± j9.761
0.05556π (10°)	-0.253 ± j2.882 -0.061 ± j3.197	-0.287 ± j6.668	-0.466 ± j9.036 -0.609 ± j9.731
0.08333π (15°)	-0.248 ± j2.892 -0.083 ± j3.170	-0.260 ± j6.663	-0.467 ± j9.064 -0.628 ± j9.677
0.11111π (20°)	-0.240 ± j2.906 -0.110 ± j3.133	-0.228 ± j6.657	-0.472 ± j9.104 -0.639 ± j9.597
0.13889π (25°)	-0.231 ± j2.924 -0.141 ± j3.088	-0.198 ± j6.651	-0.482 ± j9.153 -0.633 ± j9.494
0.16667π (30°)	-0.220 ± j2.946 -0.173 ± j3.035	-0.176 ± j6.646	-0.502 ± j9.207 -0.599 ± j9.380
0.19444π (35°)	-0.206 ± j2.973 -0.204 ± j2.978	-0.167 ± j6.644	-0.532 ± j9.261 -0.538 ± j9.269
0.19591π (35.26°)	-0.205 ± j2.975 -0.205 ± j2.975	-0.167 ± j6.644	-0.534 ± j9.264 -0.534 ± j9.264
0.22222π (40°)	-0.191 ± j3.005 -0.231 ± j2.917	-0.176 ± j6.645	-0.573 ± j9.307 -0.458 ± j9.178
0.25000π (45°)	-0.174 ± j3.043 -0.253 ± j2.859	-0.210 ± j6.646	-0.616 ± j9.334 -0.375 ± j9.118
0.27778π (50°)	-0.155 ± j3.087 -0.270 ± j2.795	-0.272 ± j6.641	-0.647 ± j9.338 -0.305 ± j9.095
0.30556π (55°)	-0.135 ± j3.139 -0.282 ± j2.739	-0.363 ± j6.616	-0.647 ± j9.330 -0.268 ± j9.107
0.33333π (60°)	-0.114 ± j3.200 -0.288 ± j2.687	-0.471 ± j6.555	-0.608 ± j9.328 -0.287 ± j9.142
0.36111π (65°)	-0.092 ± j3.273 -0.289 ± j2.641	-0.571 ± j6.449	-0.532 ± j9.353 -0.376 ± j9.167
0.38889π (70°)	-0.070 ± j3.362 -0.287 ± j2.603	-0.636 ± j6.311	-0.430 ± j9.427 -0.521 ± j9.128
0.41667π (75°)	-0.049 ± j3.476 -0.280 ± j2.576	-0.652 ± j6.168	-0.312 ± j9.570 -0.644 ± j9.001
0.44444π (80°)	-0.029 ± j3.637 -0.269 ± j2.564	-0.624 ± j6.039	-0.190 ± j9.821 -0.680 ± j8.847

# indicates double degeneracy for these zero mode poles

the same natural frequencies as would be determined for the appropriate bent wire configuration. (Note that the full-wave, second-harmonic mode natural frequency is not the same as that of the bent wire configuration.)

It is informative and enlightning to observe the nature of the coupling of the various natural modes to the individual geometrical structures as a function of the specific electromagnetic excitation scenario. This information helps in understanding which set of excitation conditions contributes to the existence of the various crooked modes and zero modes which are set up on the scattering structures. For example, coupling coefficients given by previous investigators [1,2,4] have shown that the fundamental natural mode of the isolated thin wire is excited by broadside incidence ($\theta_p = \pi/2$, $\phi_p = 0$, $\theta_{inc} = \pi/2$, $\phi_{inc} = \pi/2$, whereas the second harmonic mode (full-wave resonance) is not excited by this broadside incidence. Data given in Figures 5a-5d for the planar symmetric tri-arm geometry indicate that for excitation arriving at the incident angle and incident polarization where the exciting electric field is orthogonal to arm 1, no current is induced on arm 1 whereas non-zero currents may exist on arms 2 and 3. This situation was previously designated in Figure 3a as the "zero mode" configuration for the planar symmetric tri-arm. The current mode where non-zero currents exist on all three arms simultaneously (coupling coefficients as shown in Figure 3b) may be designated as a type of "crooked mode" similar to that found in the planar and nonplanar tetra-arm (crossed wire) cases. In this case, component "crooked mode" currents flow from arm 2 and arm 3 onto arm 1. Note that the amplitudes of the natural mode functions in Figure 3b display the superposition of these two "crooked mode" components quite clearly.

The coupling coefficients for the planar symmetric tetra-arm (planar perpendicular symmetric crossed wires) scatterer are shown in Figures 6a-6d. As has been discussed already, the coupling coefficients which produce the "zero mode" and the "crooked mode" distributions are clearly demonstrated. It is also apparent that this configuration does not lend itself to a geometrical decomposition into a pair of 90° bent wires. This can be explained since there is no conceivable excitation which would induce currents on any two mutually orthogonal arms without also producing current on the other mutually orthogonal arms, i.e. superpositions of "crooked modes" and "zero modes" will not yield currents with this nature.

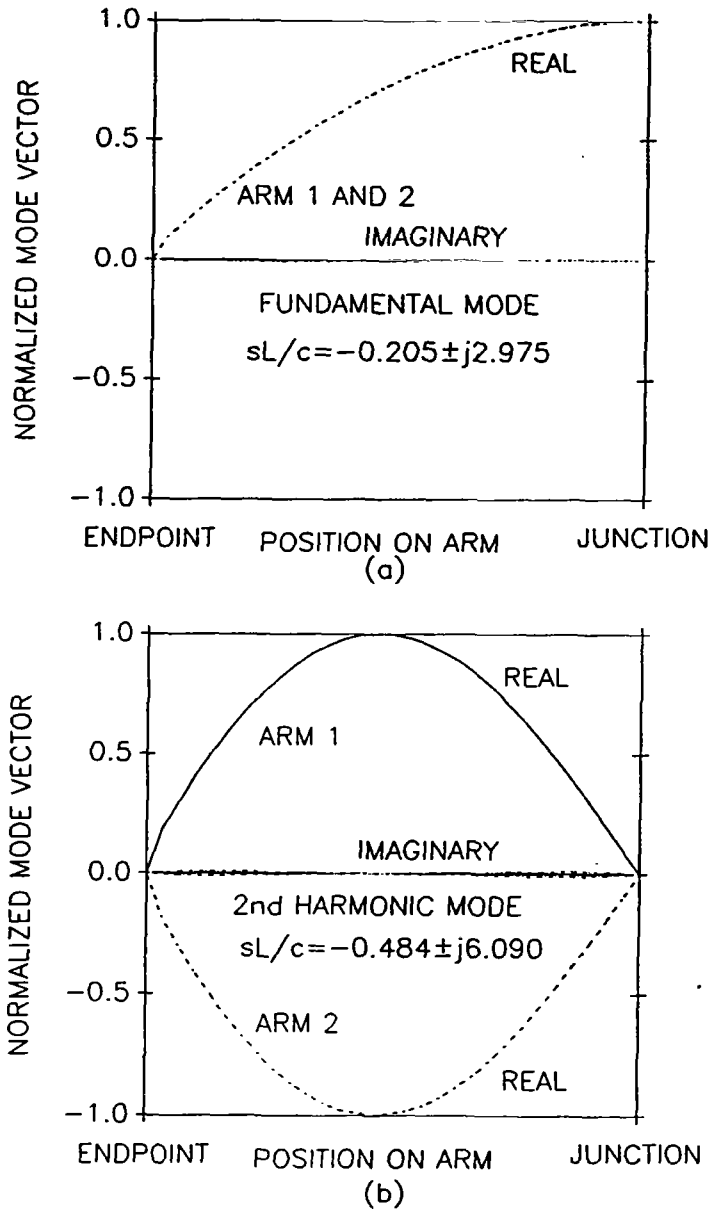

Figure 2. Natural Mode Functions for Isolated Bent Wire ($\xi = 109.47°$) : (a) Fundamental Mode (sL/c = -0.205 ± j2.975) and (b) 2nd Harmonic Mode (sL/c = -0.484 ± j6.090).

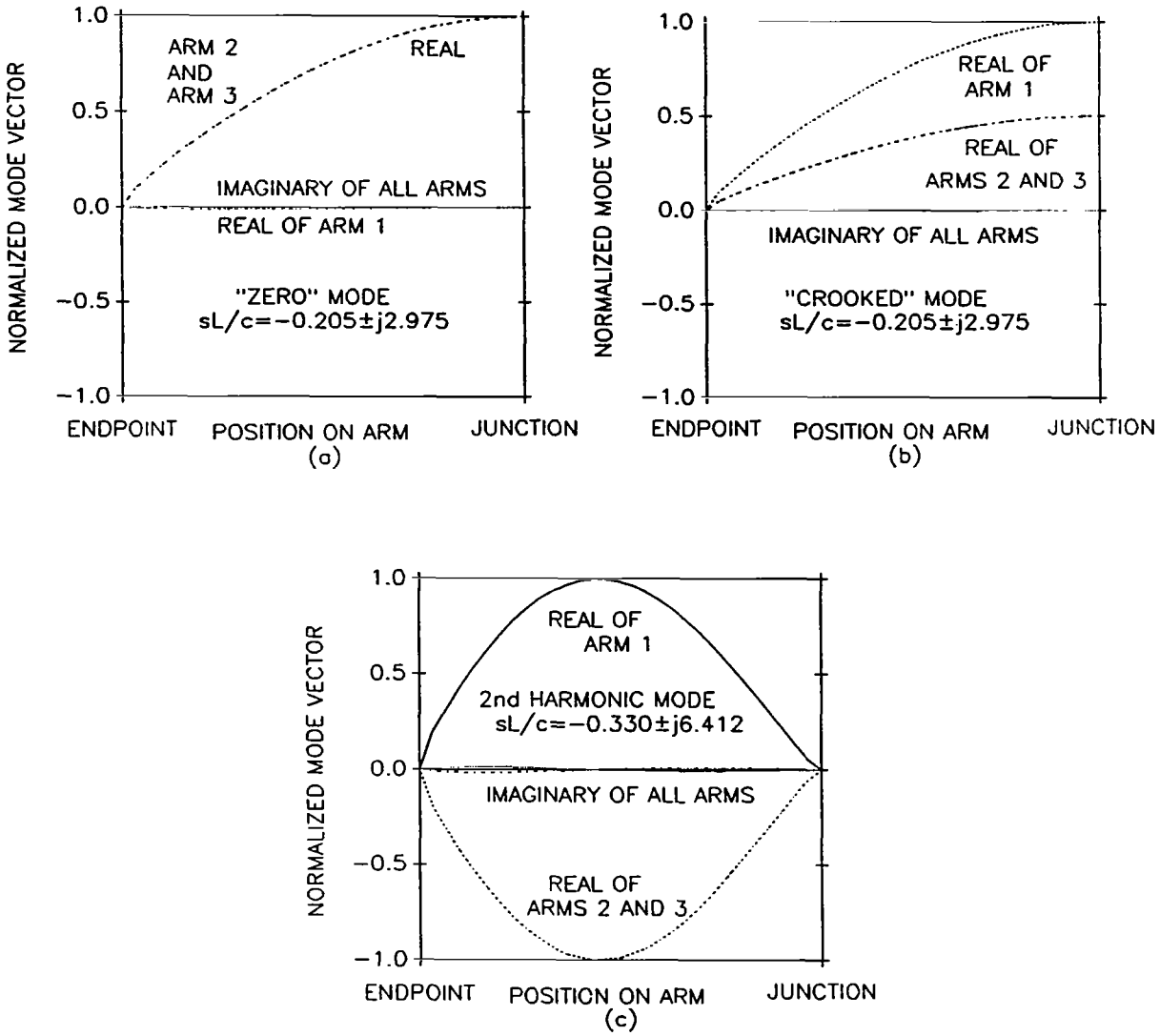

Figure 3. Natural Mode Functions for Nonplanar Tri-Arm Scatterer ($\xi = 109.^{\circ}47$) : (a) "Zero" Mode ($sL/c = -0.205 \pm j2.975$), (b) "Crooked" Mode ($sL/c = -0.205 \pm j2.975$), (c) 2nd Harmonic Mode ($sL/c = -0.330 \pm j6.412$).

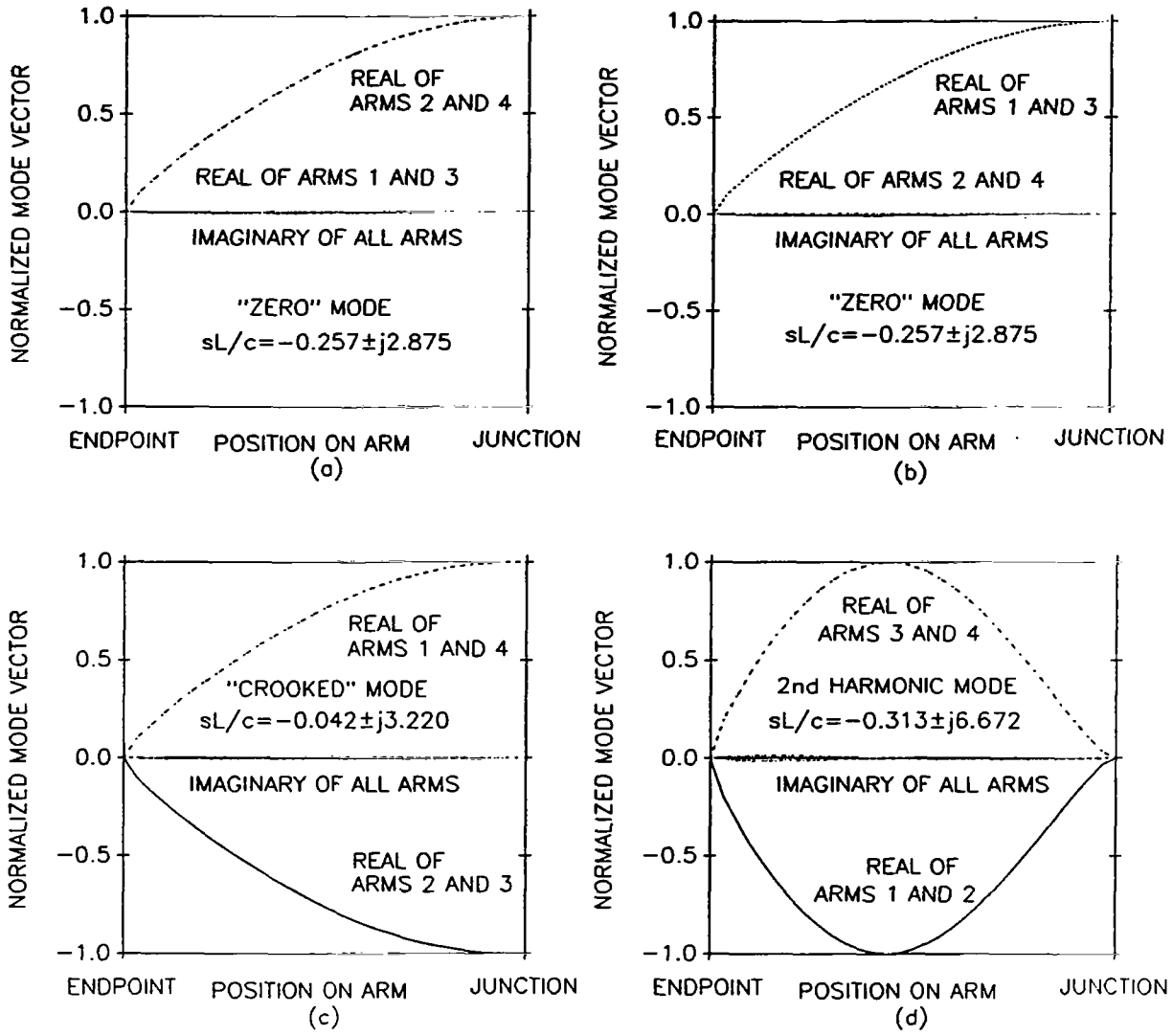

Figure 4. Natural Mode Functions for Planar Tetra-Arm Scatterer ($\xi = 90^\circ$) : (a) "Zero" Mode ($sL/c = -0.257 \pm j2.875$), (b) "Zero" Mode ($sL/c = -0.257 \pm j2.875$), (c) "Crooked" Mode ($sL/c = -0.042 \pm j3.220$), (d) 2nd Harmonic Mode ($sL/c = -0.313 \pm j6.672$).

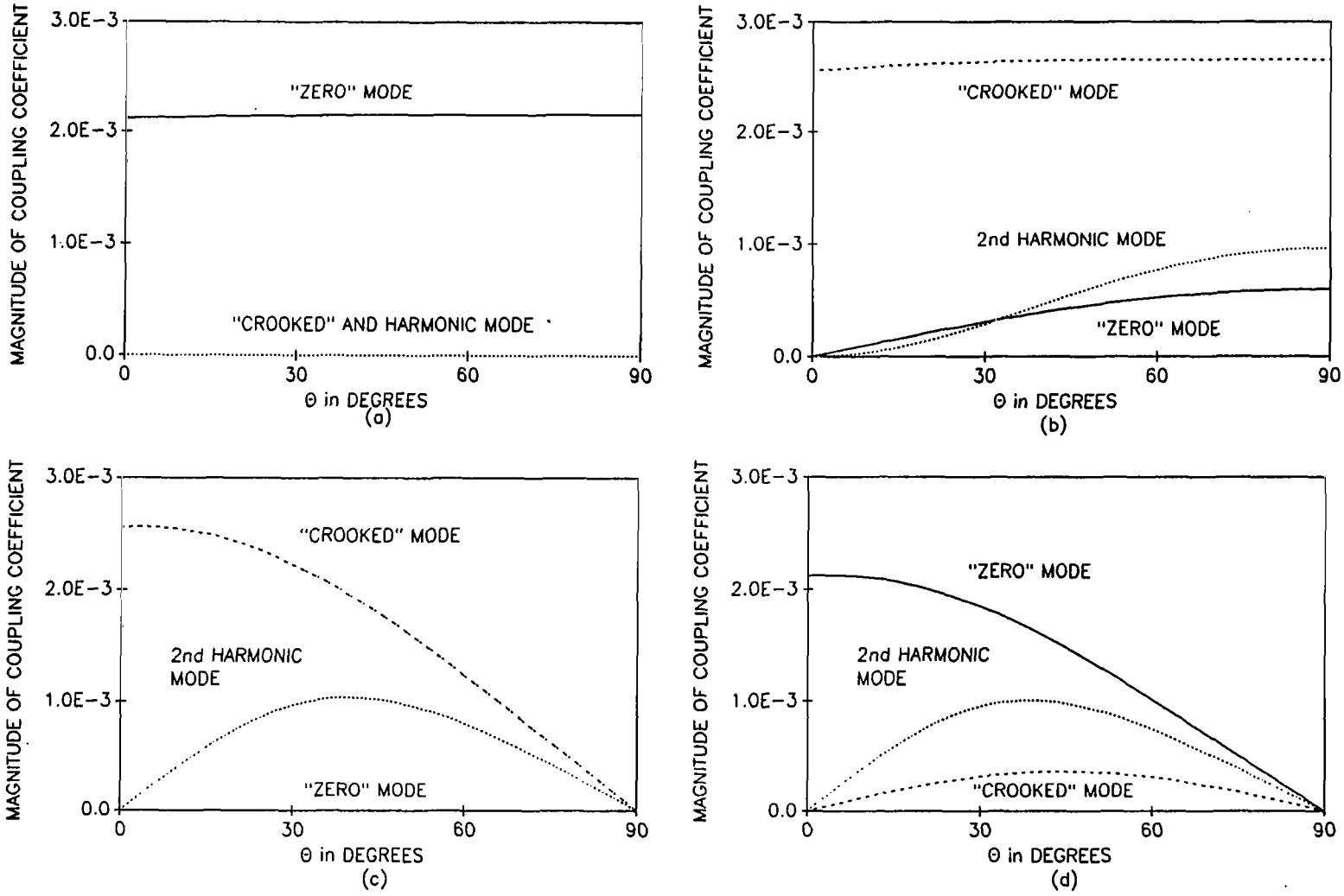

Figure 5. Coupling Coefficients versus θinc for Planar Tri-Arm Scatterer ($\xi = 120^\circ$) : (a) ϕ-polarization (incidence in the $\phi = 0$ plane), (b) ϕ-polarization (incidence in the $\phi = 90^\circ$ plane), (c) θ-polarization (incidence in the $\phi = 0$ plane), (d) θ-polarization (incidence in the $\phi = 90^\circ$ plane).

Two other geometries which yield interesting sets of coupling coefficients are the nonplanar symmetric tri-arm and the nonplanar symmetric tetra-arm. Figures 7a-7d and 8a-8d present these coefficients for the cases which excite the "zero mode" and "crooked mode" components, respectively. Since the "zero mode" case is essentially just that of an isolated bent wire, it is expected that the natural frequencies and associated mode functions are just those already given for the arbitrarily bent wire (the first entry in the second and fourth columns of Table 2.) Note that the situation given in Table 1, Case (V), #3, #4, #9, and #10, and Table 2, pivot angle of 45°, represents three mutually orthogonal wires and a pair of mutually orthogonally 90° bent wires, respectively. In each of these two cases it is possible to excite "zero mode" currents on two of the arms without exciting currents on the third or third and fourth arms, respectively. Thus both of these structures have natural frequencies and natural modes which are identical to the isolated 90° bent wire.

It should be pointed out that the coupling coefficients for the Case II configuration (the isolated bent wire) are inherently included in the coefficients previously presented for the planar and nonplanar symmetric tri-arm configurations where the existing natural mode is the "zero mode".

IV. Conclusions

In the preceding sections SEM parameters for several different geometrical scatterers have been presented. Various commonalities which inherently exist in these SEM parameters have been delineated. The relationships between these various parameters and the pertaining electrical and geometrical conditions have been presented and discussed. It is the opinion of the authors that additional insight into the fundamental nature of scatterers such as were addressed in this limited analysis and enhanced utility of observations such as these presented here may be useful to other investigators who proceed along similar lines of investigation for more complicated (and/or more practical) scattering or radiating antenna geometries.

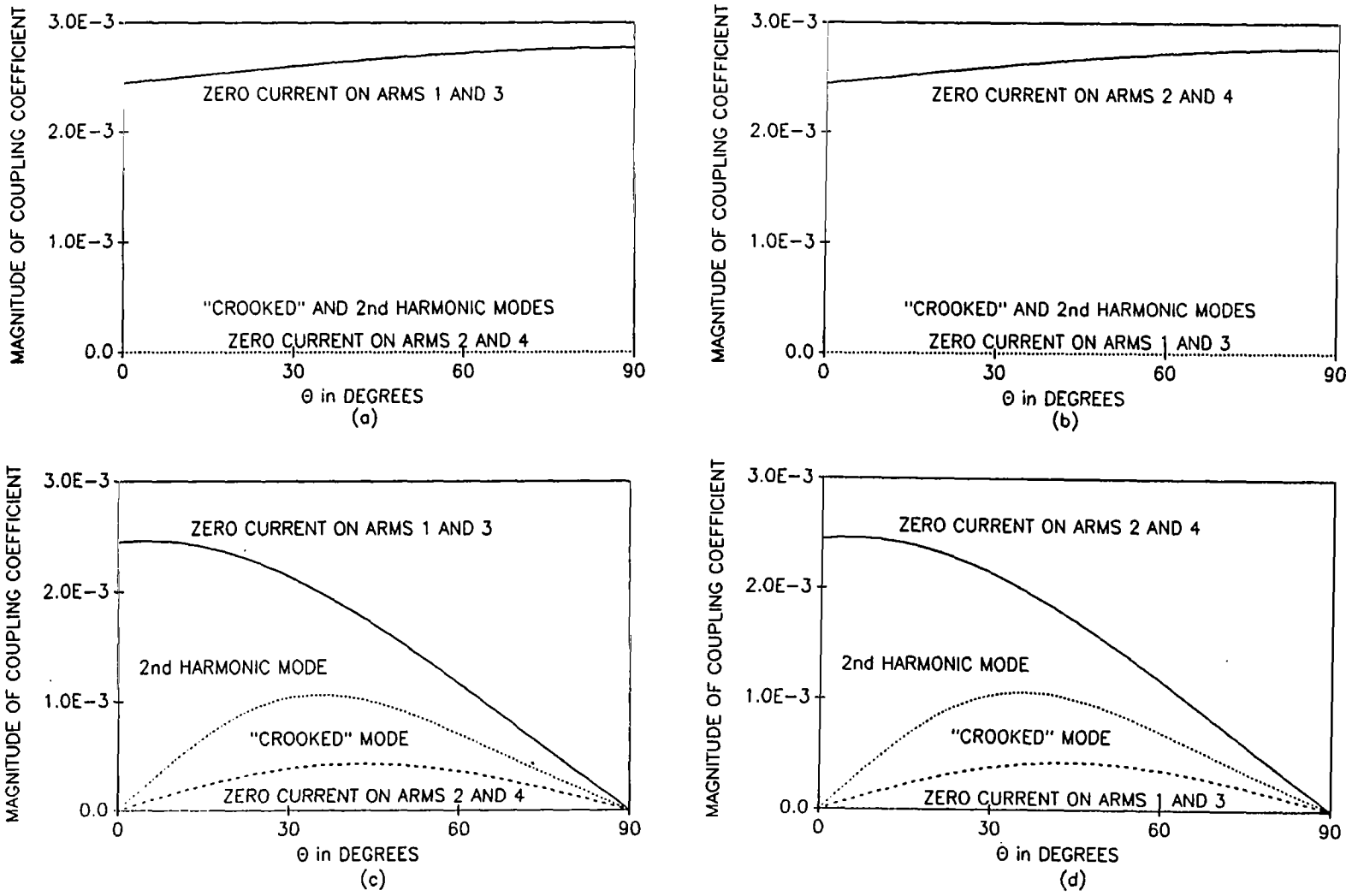

Figure 6. Coupling Coefficients versus θinc for Planar Tetra-Arm Scatterer ($\xi = 90^\circ$) : (a) ϕ-polarization (incidence in the $\phi = 0$ plane), (b) ϕ-polarization (incidence in the $\phi = 90^\circ$ plane), (c) θ-polarization (incidence in the $\phi = 0$ plane), (d) θ-polarization (incidence in the $\Phi = 90^\circ$ plane).

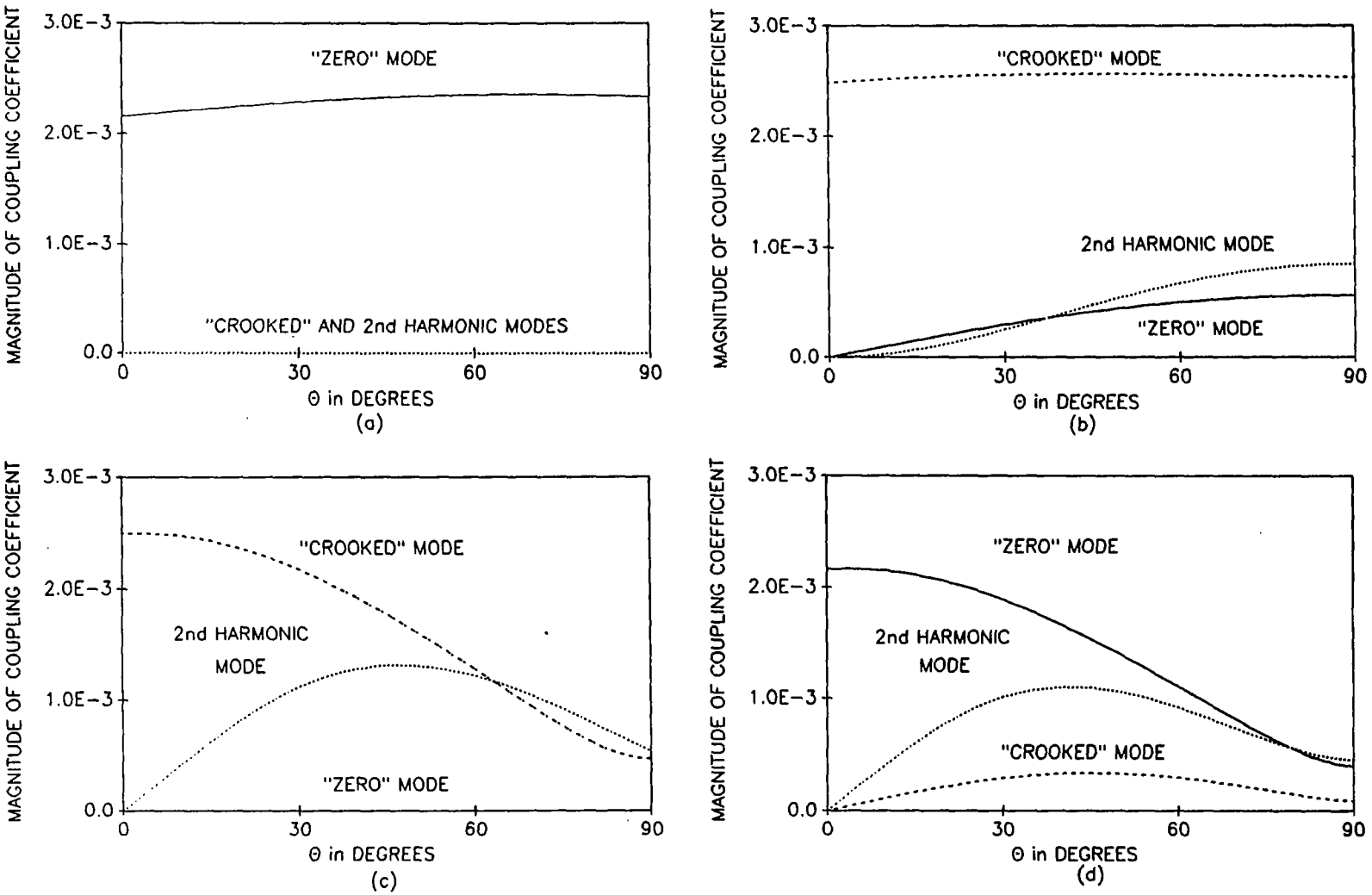

Figure 7. Coupling Coefficients versus θinc for Nonplanar Tri-Arm Scatterer ($\xi = 109.47^\circ$) : (a) ϕ-polarization (incidence in the $\phi = 0^\circ$ plane), (b) ϕ-polarization (incidence in the $\phi = 90^\circ$ plane), (c) θ-polarization (incidence in the $\phi = 0^\circ$ plane), (d) θ-polarization (incidence in the $\phi = 90^\circ$ plane).

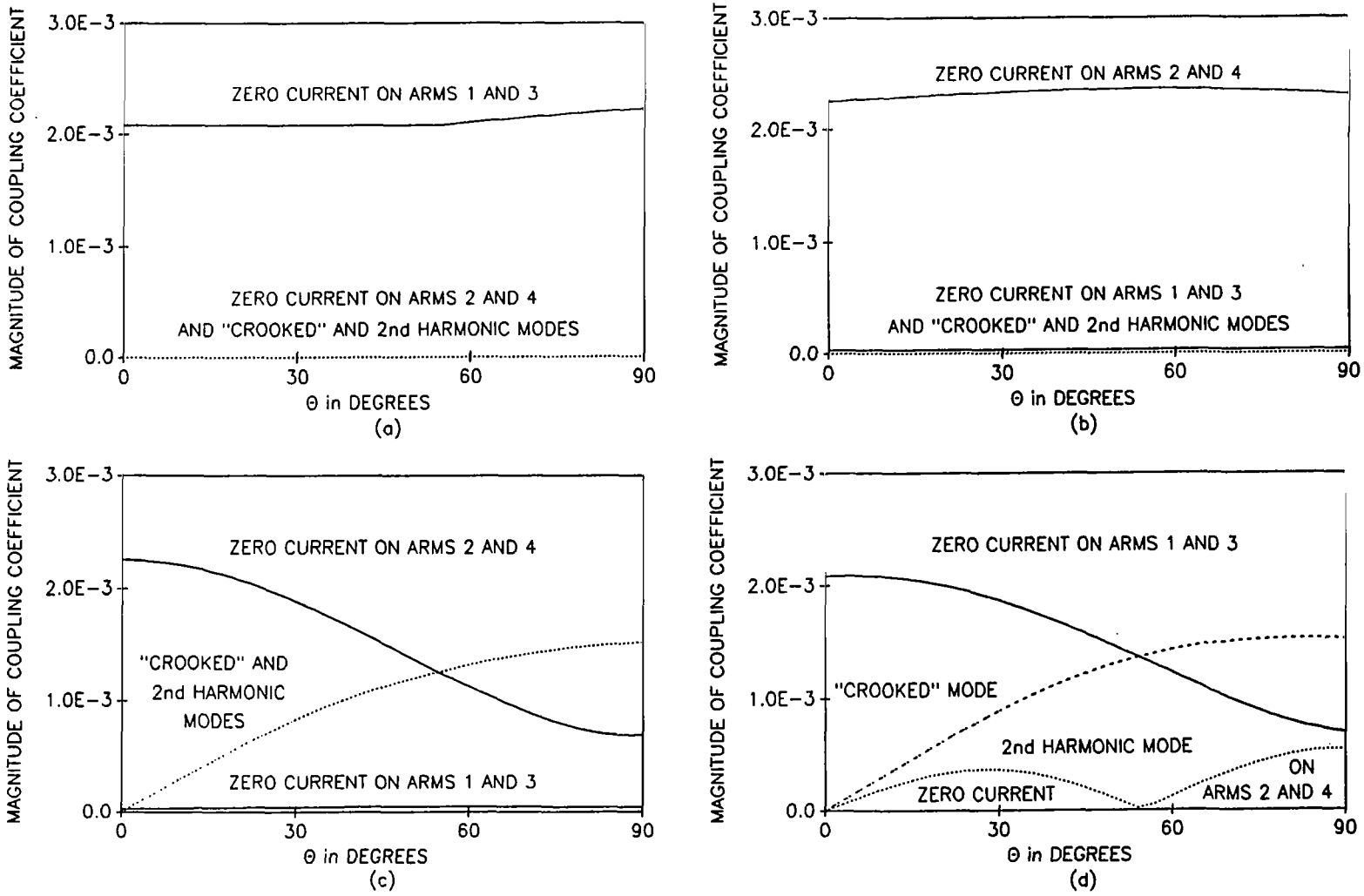

Figure 8. Coupling Coefficients versus θinc for Nonplanar Tetra-Arm Scatterer (ξ=109.47°): (a) ϕ-polarization (incidence in the ϕ = 0° plane), (b) ϕ-polarization (incidence in the ϕ = 90° plane), (c) θ-polarization (incidence in the ϕ = 0° plane), (d) θ-polarization (incidence in the ϕ = 90° plane).

REFERENCES

1. F. M. Tesche, "On the Analysis of Scattering and Antenna Problems Using the Singularity Expansion Technique," Interaction Note 102, April 1972. (Also in IEEE Trans. Ant. Prop., Vol. AP-21, No. 1, pp. 53-62, January 1973.)
2. D. R. Wilton and K. R. Umashankar, "Parametric Study of an L-Shaped Wire Using the Singularity Expansion Method," Interaction Note 152, November 1973.
3. L. S. Riggs and R. G. Smith, "Efficient Current Expansion Modes for the Tripole Frequency Selective Surface," IEEE Trans. Ant. Prop., Vol.AP-36, No. 8, August 1988 (to appear).
4. T. T. Crow , B. D. Graves, and C. D. Taylor, "The Singularity Expansion Method as Applied to Perpendicular Crossed Wires," Interaction Note 161, October 1973. (Also in IEEE Trans. Ant. Prop., Vol AP-23, No.4, pp. 540-546, July 1975.)
5. R. F. Harrington, Field Computation by Moment Methods, Macmillan, 1968.
6. C. E. Baum, "Emerging Technology for Transient and Broad-Band Analysis and Synthesis of Antennas and Scatterers,"Interaction Note 300, November 1976. (Also in Proc. IEEE, Vol. 64, pp. 1598-1616, November 1976.)
7. T. T. Crow, C. D. Taylor, and M. Kumbale, "The Singularity Expansion Method Applied to Perpendicular Crossed Wires over a Perfectingly Conducting Ground Plane," IEEE Trans. Ant. Prop., Vol. AP-27, No. 2, pp. 249-252, March 1979.
8. E. L. Pelton and B. A. Munk, "Scattering from Periodic Arrays of Crossed Dipoles," IEEE Trans. Ant. Prop., Vol. AP-27, No.3, pp. 323-330, May 1979.
9. C. E. Baum, "Interaction of Electromagnetic Fields with an Object Which Has an Electromagnetic Symmetry Plane," Interaction Note 63, March 1971.
10. C. E. Baum, "A Priori Application of Results of Electromagnetic Theory to the Analysis of Electromagnetic Interaction Data," Interaction Note 444, February 1985. Also in Radio Science, Vol. 22, No. 7, pp.1127-1136, December 1987.
11. C. E. Baum, T. H. Shumpert, and L. S. Riggs, "Perturbation of the SEM-Pole Parameters of an Object by a Mirror Object," Sensor and Simulation Note 309, September 1987. Also in Electromagnetics, Vol. 9, No. 1, 1989.